Spectrum of Engineering Sciences
ISSN (e) 3007-3138 (p) 3007-312X Volume 3, Issue 3, 2025

IN-SITU ELEMENTAL DETECTION IN TOBACCO AND ASH BY LASER INDUCED BREAKDOWN SPECTROSCOPY: IMPLICATIONS FOR HUMAN HEALTH AND ENVIRONMENTAL SUSTAINABILITY

Nimra Shahzad[*1], Madma Habib[2], Yasir Ali[3]

[*1]*Laser and Optronics Centre , Department of Physics, University of Engineering and Technology-Lahore Pakistan*
[2]*Department of Chemistry, University of Sargodha, Sargodha Pakistan*
[3]*Department of Computer Science Quaid E Awam University of Engineering Scinece and Technology Nawabshah*

[*1]nimra.zaad04@gmail.com, [2]madmahabib01@gmail.com, [3]yasirali988@gmail.com

DOI: https://doi.org/10.5281/zenodo.15043887

Keywords
LIBS, Tobacco, Cigarette Ash, Toxic Elements, Mc Whirter Criteria.

Article History
Received on 10 February 2025
Accepted on 10 March 2025
Published on 18 March 2025

Corresponding Author: *

Abstract

Laser induced breakdown spectroscopy (LIBS) is a versatile technique that is used to determine elemental composition in different samples. It is simple and fast multi-elemental analysis technique which provides potential tool in situ chemical analysis with high resolution, better limit of detection (LOD) and is cost efficient. Smoking tobacco in cigarettes amplifies the risk of growing certain diseases such as cancer, heart disease, stroke, lung diseases, diabetes, and chronic obstructive pulmonary disease (COPD), which includes emphysema and chronic bronchitis. About 80% of lung cancer as well as about 80% of all lung cancer deaths are due to smoking. Smoking tobacco is a considerable source of consuming several harmful and toxic elements that are unhealthy for human body. The presence of some toxic elements causes serious health concern to active as well as to passive smokers. In the present study, we employ LIBS technique to identify and detect toxic and harmful elements in tobacco and ash from four popular Pakistani cigarette brands, ensuring human health protection, agricultural safety, and environmental sustainability. The Q-switched ND: YAG (neodymium-doped yttrium aluminum garnet) laser (λ=1064 nm) with laser energy 90 mJ and pulse duration 10 ns were used to ablate the samples. From the recorded optical emission spectra of these samples several elements were detected (Fe, Ca, Mn, Sc, Ti, Cr, Sc, Sr and Ni) among which Chromium Cr, Nickel Ni and Strontium Sr are highly toxic elements. Furthermore, the presence of toxic and heavy metals in ash could be significant contributor to metal load in soil as well as for human body. We calculated the electron temperature (Te) by the Boltzmann Plot Method from the spectroscopic analysis of the transition lines of Fe-I (iron). Stark Broadening Method was used to determine electron number density (Ne) from the transition line of Fe-I at 422.413 nm and 649.25 nm for tobacco and ash sample respectively, under the assumption of local thermodynamic equilibrium. The present results demonstrate that LIBS is a powerful diagnostic tool for effectively tracing harmful and toxic elements in various solid samples, facilitating the development of protective environmental measures.

INTRODUCTION

The use of tobacco products, particularly cigarettes, is a major factor in developing serious health conditions, such as lung disease, cancer, and other respiratory disorders [1]. It also causes stroke, heart disease and diabetes. It also uplifts possibility for certain eye diseases and tuberculosis [2]. It is also one of the prime reason of death in human being [3]. According to Action on Smoking and Health (ASH) around more than one billion people that smoke, 80% of them are from LMICs (low and middle income countries), and that number is continuously increasing [4]. Tobacco plants easily absorb certain metals from soil such as nickel and in particular cadmium in leaves [5]. Cadmium is basically unsafe and poisonous element, which is absorbed by herbaceous plants and is later conveyed to humans by inhaling cigarette [6]. Metal concentrations in tobacco are also affected by soil type [7], different insecticides are used to increase yield of tobacco crops which contain toxic compounds and further chemicals that are used to increase the flavor and to fabricate cigarette that catch fire easily [8]. It is becoming increasingly necessary to find out if cigarette consumed contain extent amount of metals or not.

Different techniques can be used to analyze sample for heavy metals for example graphite furnace atomic absorption spectroscopy (GFAAS) [9] after microwave-assisted technique but for this method if sample is in solid form it must first bring into solution before the analysis [10]. Another method used to determine metal concentration is Energy Dispersive X-ray Spectroscopy (EDX)
[11][12]. It provides quantitative elemental analysis. Analysis of this technique utilize thin sample. Elements with low atomic number are unable to notice by some Energy Dispersive X-ray Spectroscopy [13][14]. Neutron Activation Analysis is a most sensitive technique to detect elements in a material sample [15] but for this technique large amount of material is required and sample becomes radioactive. This technique is also time consuming [16].

Laser-induced Breakdown Spectroscopy (LIBS) is an appropriate technique for quantitative study of metallic elements [15]. With LIBS technique any type of sample can be analyzed whether solid, liquid or gas [17]. LIBS technique is easy, straightforward, uncomplicated and fast which provides potential tool in situ chemical analysis with high resolution, better limit of detection (LOD) and is cost efficient [8]. Moreover, time consuming sample preparation is not required, which is preferable for a number of applications [18].

During the process of smoking various metal load left in ash. The aim of this research work is the detection of toxic and other elements in tobacco and its ash of different cigarette brands and to calculate different plasma parameters by applying LIBS technique.

2. Materials and Methods

2.1. Sample Preparation

The tobacco and ash samples were obtained from four different cigarettes brands that are commercially available including Capstan, Gold Flake, Gold Leaf, and Morven named as S_1, S_2, S_3, and S_4, respectively. The choice of choosing these brands is due to their popularity and high selling ratio in Pakistan. From each individual brand the tobacco was set apart by taking away the filtration material, tipping paper and cigarette paper. The tobacco samples are in the large grain size due to natural texture of the dry tobacco leaves and it is difficult to generate an efficient plasma for accurate analysis. For the stability of plasma, sample is changed into fine powdered form. For this purpose, the tobacco samples are grinded into fine powder by using a manual grinder. For ash, tobacco was first burned and ash were collected in a petri dish. Since ash was already in a fine powder state hence no need to grind it. Figure 1. shows the samples of tobacco, grinded tobacco and of tobacco ash before converting into pallets.

Fig. 1. Sample material: (a) Cigarettes, (b) Separated tobacco grain from a cigarette, (c) Grinded tobacco for palletization, (d) Tobacco ash for palletization.

With the help of hydraulic press, tobacco and its ash were converted into round shaped pellets with thickness approximately 5 mm and diameter 12 mm by exerting 10 psi pressure for 15 minutes. It was not necessary to add any adhesive material since both tobacco and its ash confined efficiently by itself.

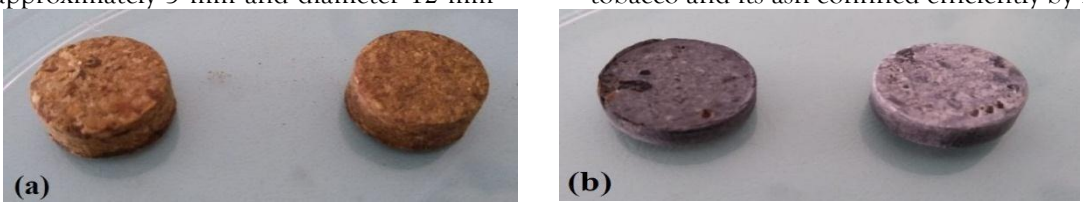

Fig.2. Sample in pellets form after using Hydraulic press: (a) Palletized tobacco cigarettes for LIBS analysis, (b) Palletized tobacco ash for LIBS analysis.

2.2. LIBS SYSTEM

The photographic view of experimental LIBS set-up is shown in **Fig. 3**. In the present work, the LIBS set-up comprises of Nd: YAG Q-switched laser with wavelength of 1064 nm, laser energy of 90 mJ, laser frequency of 10 Hz and pulse duration of 10 ns were used to ablate the target material [8].

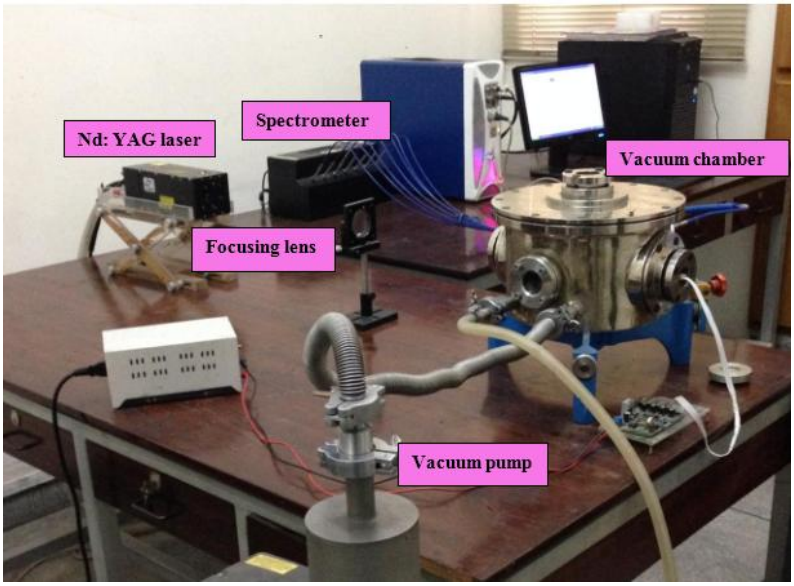

Fig. 3. Photographic view for LIBS system.

The samples were placed on a rotating stage which gives new position of the target for each laser shot and minimize the generation of deep craters. This enhance the reproducibility of mass ablation by abstaining from the non-homogeneity of the sample target as well as precise measurement of atomic emission lines were obtained. A laser fluence of 63 J/cm^2 was applied to the sample to produce a plasma plume of sufficient intensity for accurate LIBS analysis. The chamber had been evacuated to 10^{-3}

torr base pressure. Chamber then filled up with argon gas at a pressure of 10 torr to enhance the optical emission. A focusing lens with focal length 50 cm applied to direct laser pulse upon the target material. A window was opened on the inner side of the chamber at which a fibre collimator was fixed, which captured radiations from plasma spark generated on the sample surface with the help of collecting lens of focal length 5 cm. In order to minimize breakdown in argon gas, samples were positioned by a length less than the focal length of the focusing lens. Figure 4. Shows the schematic diagram for the LIBS set-up.

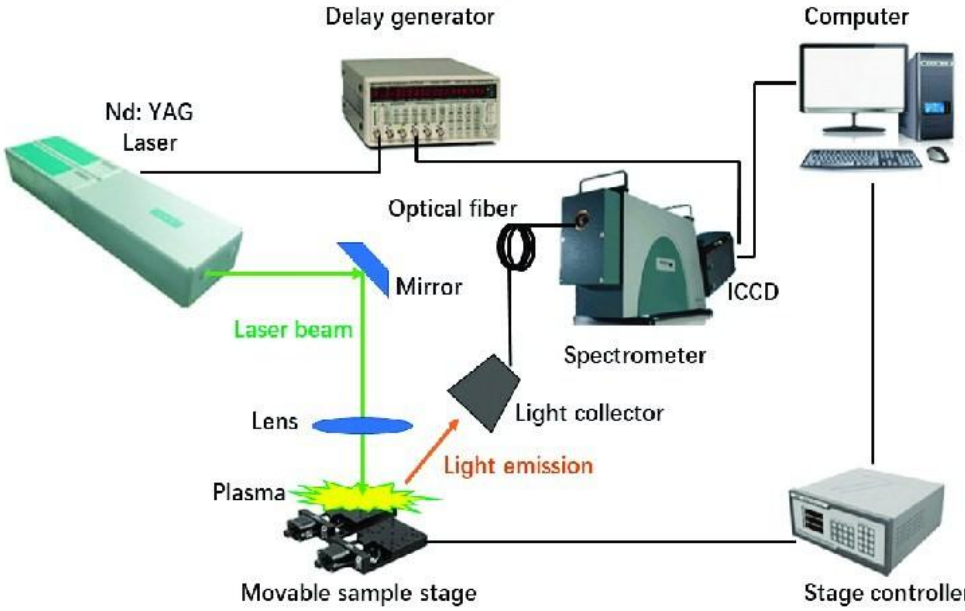

Fig. 4. Schematic diagram for LIBS system. [19]

2.3. Data Acquisition and Analysis

In the present work, emission spectra from the plasma of tobacco and its ash were collected and analyzed by LIBS 2500 plus (LIBS spectrometer system). It comprises of fibre bundle including seven linear silicon charge coupled device (CCD) array detectors, covering a wide wavelength range of 200-980 nm for the analysis with spectral resolution of 0.1 nm.

The laser optical emission spectroscopy has been used to analyze different elements present in the different samples of tobacco and its ash. The LIBS analysis identified numerous elements across a broad spectral range (400-800nm), with corresponding emission intensities and wavelengths. All the elements which are detected are labelled by NIST DATABASE [19]. Different number of laser shots falls on target material following similar conditions such as distance from sample to laser, laser frequency, laser energy and pulse duration. Spectral emission attained from laser induced plasma of tobacco samples (S_1, S_2, S_3 and S_4) and corresponding ash samples (S'_1, S'_2, S'_3 and S'_4) are shown in **Fig.5(a) and Fig.5(b)** respectively. Spectroscopic database (NIST) was used to identify each individual emission line. Different elements are detected which are Fe, Ti, Cr, O, P, Si, Ni, C, Sr, Mn, Sc, Cr, W and Al.

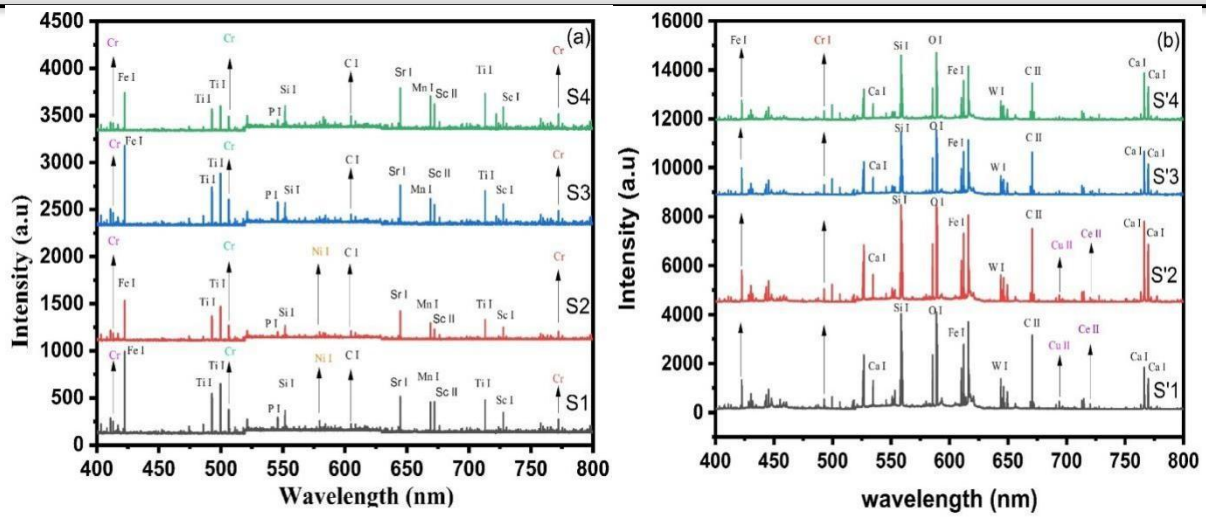

Fig.5. The optical emission spectra of all tobacco samples (a) and corresponding all ash samples (b)

The spectral analysis revealed that Iron (Fe-I) exhibited the most prominent spectral signature, with the highest number of peaks observed in both tobacco and ash samples across various wavelengths. In LIBS analysis the selection of suitable emission line is an important step for the calculation of plasma parameters. From the emission spectrum those lines were selected which contain maximum number of intensity peaks.

3. Results and Discussion

3.1. Identification of Elements

In sample S_1 and S_2, four lines of Fe-I at different wavelengths (403.32, 422.431, 474.38 and 485.83 nm) are detected. The Ti-I and Cr-I both have three lines at the wavelengths (492.83, 499.70 and 713.05 nm) and (413.21, 506.32 and 772.13 nm) respectively. One line of O-II, Sc-II, O-I, SiI, Ni-I, C-I, Sr-I, Mn-I, P-I and Sc-I are found at the wavelengths 411.02, 672.17, 521.16, 551.75, 579.60, 604.91, 644.66, 669.06, 545.83 and 727.76 nm respectively. Out of these elements Cr, Ni and Sr are toxic.

However, the spectrum of sample S_3 and S_4 have five peaks of Fe-I at different wavelengths i.e., 403.32, 422.431, 485.83, 676.30 and 721.99 nm. Ti-I and Cr-I have three lines at different wavelengths (492.83, 499.70 and 713.05 nm) and (413.21, 506.32 and 772.13 nm) respectively. One line of O-II, O-I, Sc-II, P-I, Sr-I, Mn-I, Si-I, Sc-I and C-I are also detected at the wavelengths 411.01, 521.16, 672.17, 545.83, 644.66, 669.06, 551.75, 727.76 and 604.91 nm respectively.

Among these detected elements Cr and Sr are toxic.

In the ash samples S'_1 and S'_2, Fe-I element have six emission lines at different wavelengths (403.32, 422.431, 506.33, 526.83, 612.02 and 649.25 nm). The element Ca-I have five peaks at different wavelengths (430.18, 534.74, 585.53, 766.33 and 769.75 nm). Both Si-I and Cr-II have two peaks at different wavelengths (558.62 and 646.12 nm) and (616.06 and713.063 nm) respectively. A single emission line of individual element Cr-I, P-I, Mn-I, O-I, Mn-II, W-I, Ti-I, Al-I and C-II is observed at the wavelengths 492.84, 714.71, 445.36, 588.78, 610.12, 643.81, 499.70, 433.39 and 670.65 nm, respectively. Out of these Cr is toxic element.

Ash samples S'_3 and S'_4 have six peaks of Fe-I element at different wavelengths (403.3, 422.431, 506.33, 526.83, 612.02 and 649.25 nm). Five lines of Ca-I element at different wavelengths (430.18, 534.74, 585.53, 766.33 and 769.75 nm) were present. Si-I have three lines at different wavelengths (558.62, 646.12 and 727.75 nm). Cr-II element has two lines at wavelengths 616.05 and 713.06 nm. A single peak of each individual element Mn-I, O-I, Mn-II, Cr-I, Al-I, Ti-I, C-II, P-I and W-I are detected at the wavelengths 445.36, 588.78, 610.12, 492.84, 433.39, 499.70, 670.65, 714.71 and 643.81 nm, respectively. Out of all these elements Cr is toxic.

Elements W-I and Al-I were not identified in tobacco samples but found in ash samples. More elements

are detected in ash than in tobacco which may be due to the contribution of metallic elements from cigarette wrapping paper.

3.2. Plasma Parameters

Two main parameters of plasma that is plasma temperature and electron number density are calculated by using emission spectra of Fe-I for all samples since it has greater emission intensity.

3.2.1. Electron Temperature (T_e)

In order to find the electron temperature there are two procedures:

1.Boltzmann plot method

2.Saha Boltzmann method

In this work Boltzmann Plot Method is applied to compute electron temperature and it is only for neutral atoms. However, Saha Boltzmann method is used for the atoms possessing dissimilar transition states [20].

By the Boltzmann Plot Method electron temperature is calculated by applying the given equation:

$$\ln\frac{\lambda_{ij}I_{ij}}{gA_{ij}} = \frac{E_j}{kTe} + \ln\left(\frac{N(T)}{U(T)}\right)$$

Where λ_{ij}, I_{ij}, g, A_{ij} and E_j are the transition wavelength, integrating intensity of the emission line, statistical weight of the upper state, transition probability and upper state energy, respectively.

Whereas, k, T_e, N(T) and U(T) are the Boltzmann constant, electron temperature in kelvin, total number density of neutral atoms and partition function respectively [21].

To calculate the electron temperature (T_e), the intensity of F_e (I) emission lines and their spectroscopic data as given in Table1, are used in eq.1 to draw the Boltzamnn plot. The Boltzmann plot consists of data points, that is the ln $\lambda_{ij}I_{ij}/gA_{ij}$ as a function of E_j (eV) and the linear fitting over these data points gives the slope (T_e = -1/mk), which yield the electron temperature. The calculated values of electron temperature (T_e) vary from 8728 K to 10363 K for tobacco samples, and from 8928 K to 10363 K for ash samples.

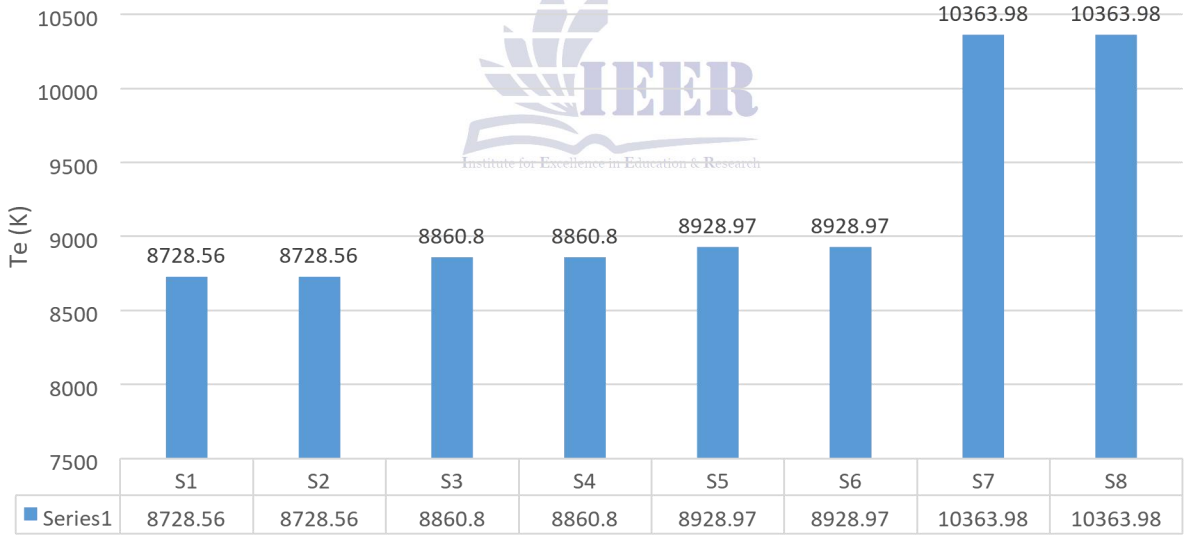

Fig.6. The bar chart of plasma temperature for all samples using Fe (I).

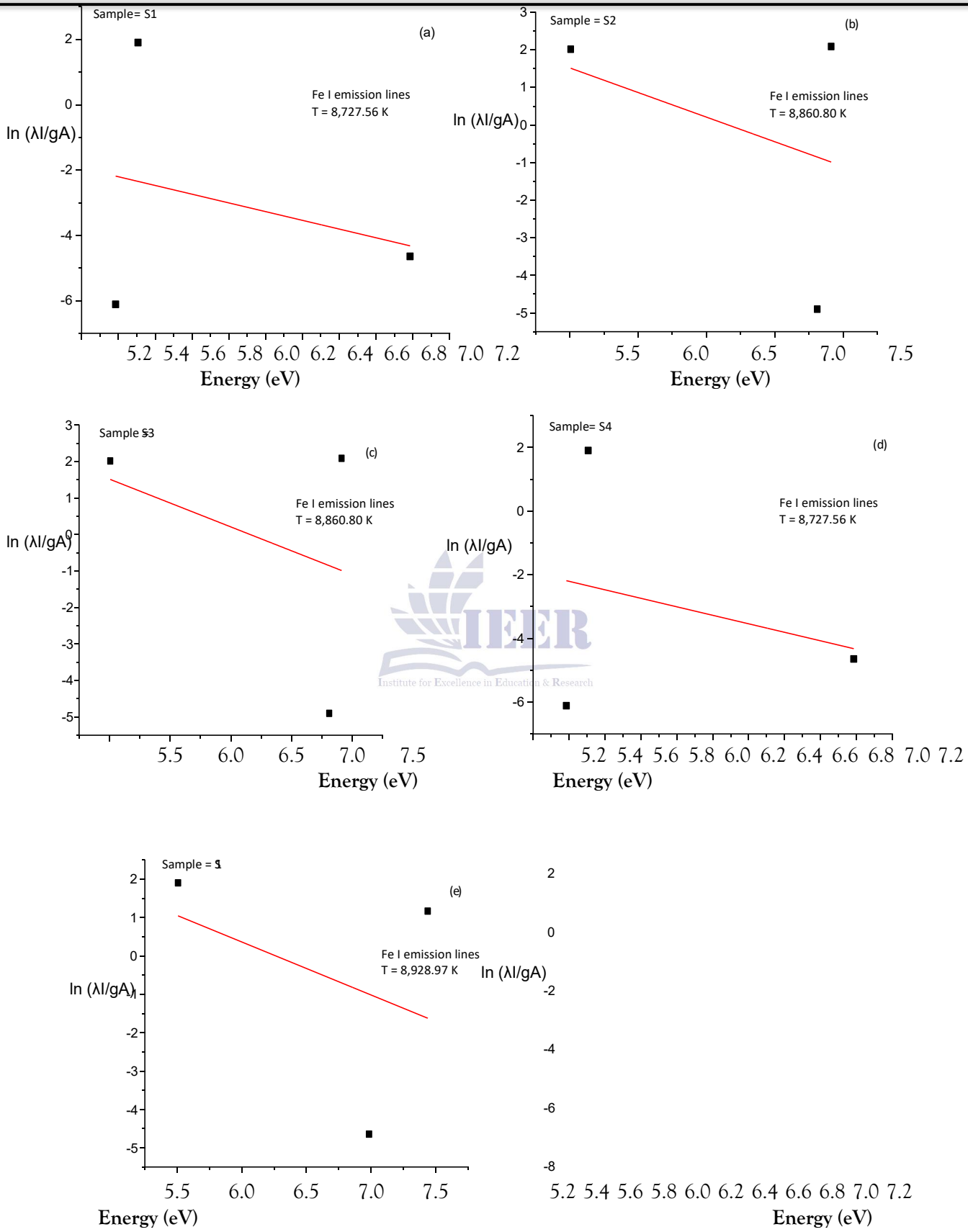

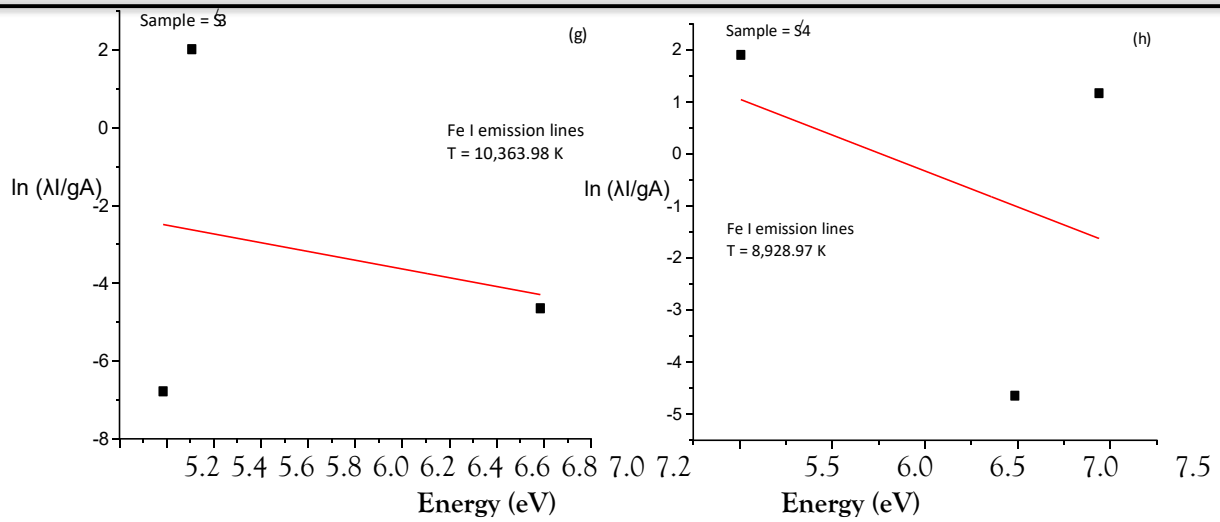

Fig.7. Linear fitting of Boltzmann plots of Fe-I emission line for all tobacco samples (a-d) and all ash samples (e-h).

Table 1. Spectroscopic parameters of Fe(I) emission lines identified in all samples.

Wavelength nm	*Upper Transition*	*Transition probability As^{-1}*	*Upper- level energy eV*	*Statistical Weight g*
403.32	3d3.2d2.4p	4.60×10^{2}	5.50677	9
422.22	3d6.5d.4s.6d.5s	5.76×10^{6}	5.38521	7
474.38	3d6.4s.4d.4d	3.61×10^{5}	6.98491	7
676.3	3d6.4s.4d.4d	2.81×10^{6}	7.31082	3
721.99	3d6.4s.6d.6p	7.21×10^{3}	7.41282	1
526.83	3d6.4s.6d.5g	6.92×10^{3}	7.43897	5
670.14	3d6.4s.4d.4d	1.04×10^{1}	7.20746	7

3.3.2. Electron Number Density (N_e)

The number density of electrons determines the degree of ionization and validates the assumption of local thermodynamic equilibrium (LTE) [23]. The electron number density is evaluated by Stark broadening method. Other broadening mechanisms such as natural broadening, pressure broadening, and Doppler broadening are negligible in comparison to Stark broadening, whereas instrumental broadening cannot be neglected.

This work uses the Fe (I) line at 422.413nm and 649.25 nm are utilized to determine electron number density for tobacco and ash samples respectively. In Fig4, the line profile is fitted with the Voigt function to get the full width at half-maximum, or FWHM ($\Delta\lambda_{1/2}$). The electron number density N_e is determined by the following equation.

$$N_e(cm^{-3}) = \left(\frac{\Delta\lambda_{1/2}}{2w}\right) \times 10^{16}$$

Where, N_e is the density of electron in cm^{-3} and ω is electron impact parameter given by following equation.

$\omega = 4.8767 \times 10^{-4} + 1.6385 \times 10^{-8} (T_e) - 1.8473 \times 10^{-13} (T_e)^2$

Where "T_e" is electron temperature [19]. The value of N_e calculated for tobacco samples S_1 and S_2 is 3.065×10^{16} cm^{-3}, and for sample S_3 and S_4 is 1.738×10^{16} cm^{-3}, for ash sample S'_1 and S'_2 it is 3.003×10^{16} cm^{-3} and for sample S'_3 and S'_4 it is 1.670×10^{16} cm^{-3}.

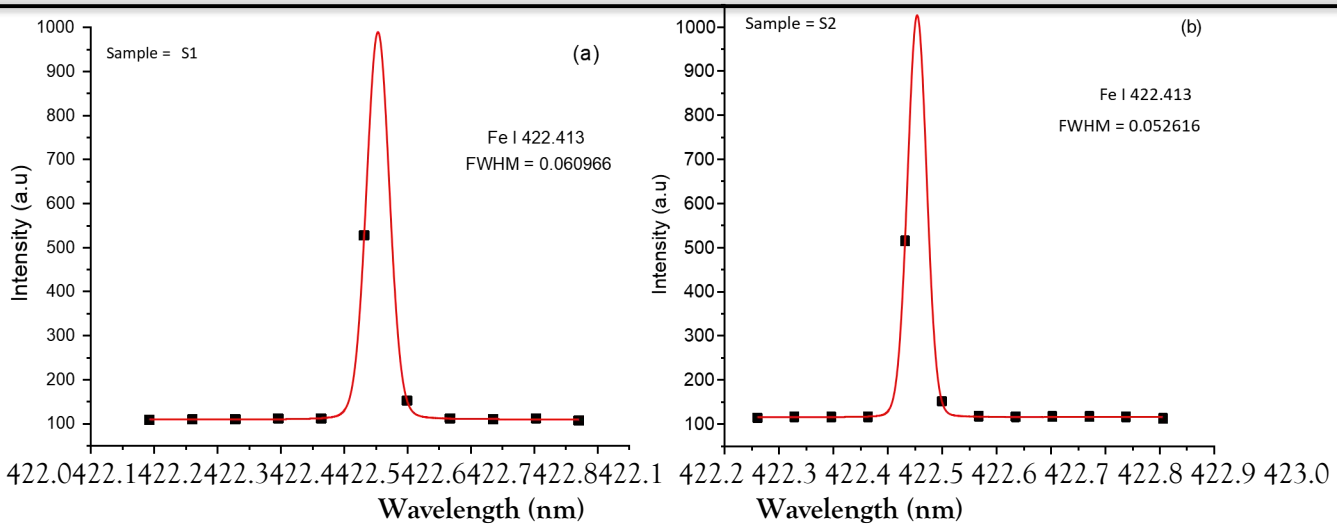
Sample = S1
(a)
Fe I 422.413
FWHM = 0.060966
Intensity (a.u)
Wavelength (nm)
Sample = S2
(b)
Fe I 422.413
FWHM = 0.052616
Intensity (a.u)
Wavelength (nm)

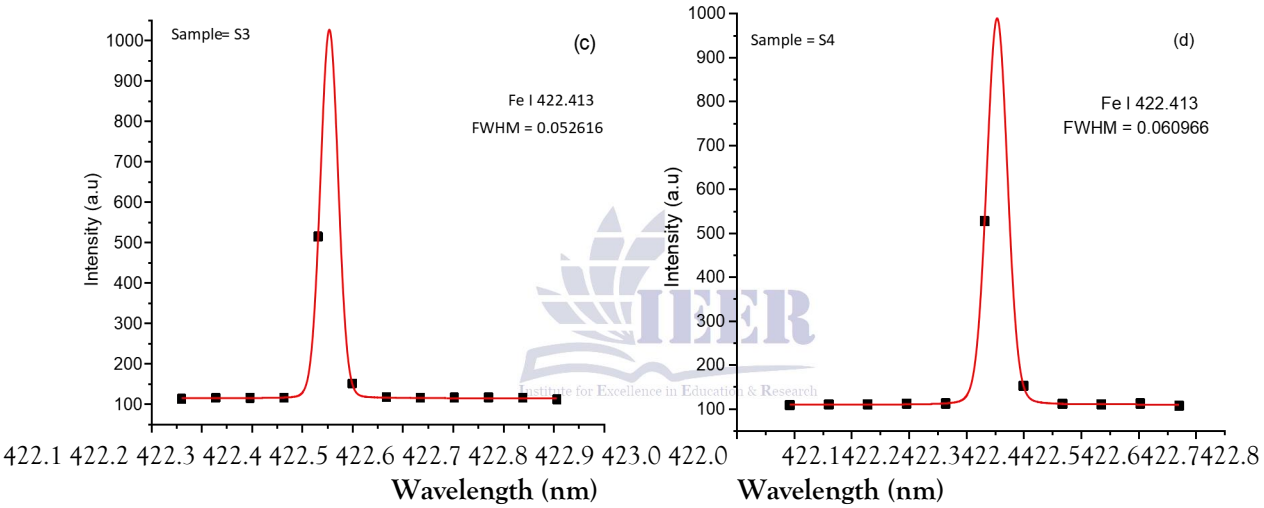
Sample= S3
(c)
Fe I 422.413
FWHM = 0.052616
Intensity (a.u)
Wavelength (nm)
Sample = S4
(d)
Fe I 422.413
FWHM = 0.060966
Intensity (a.u)
Wavelength (nm)

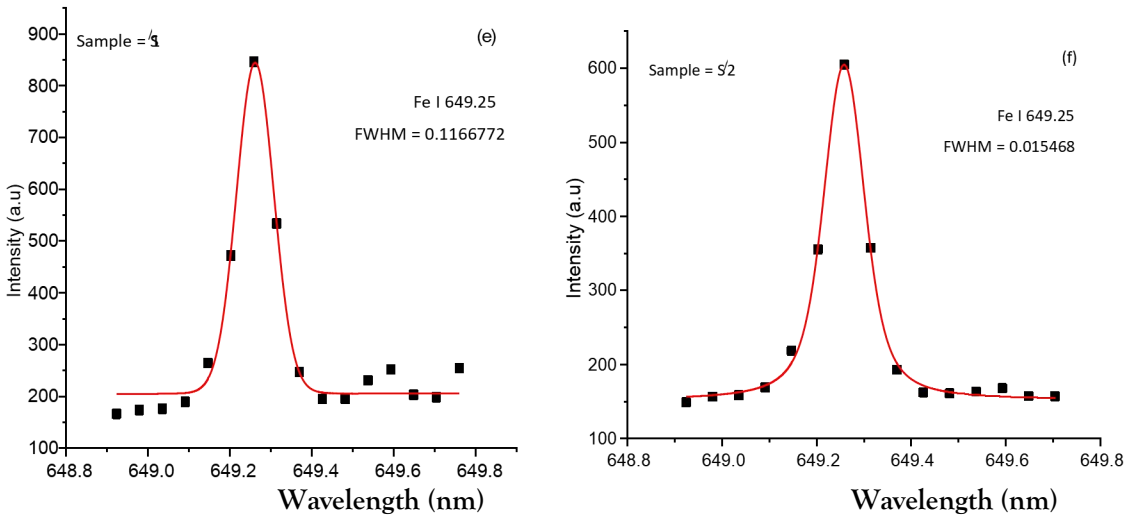
Sample = S1
(e)
Fe I 649.25
FWHM = 0.1166772
Intensity (a.u)
Wavelength (nm)
Sample = S2
(f)
Fe I 649.25
FWHM = 0.015468
Intensity (a.u)
Wavelength (nm)

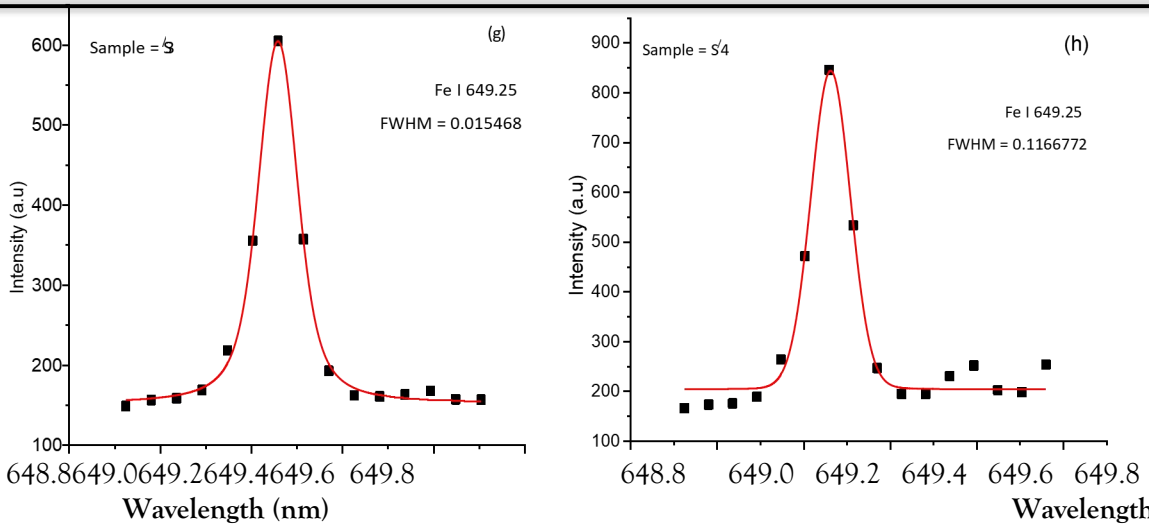

Fig.8. A voigt fitting of Fe-I line from LIBS spectra of four tobacco samples (a-d) and four ash samples (e-h).

3.3.3. Assessment of LTE Criteria

For authenticity of local thermodynamic equilibrium (LTE), Mc Whirter's criteria should be fulfilled, as given in Eq. 4:

$N_e \geq 1.6 \times 10^{12} (T_e)^{1/2} (\Delta E)^3$

Here T_e stands for electron temperature and ΔE is the maximum difference in energy from higher to lower energy states [24].

The right side of Eq 4, gives the Ne as 10^{15} cm^{-3}, which is less than the experimental value ~ 10^{16} cm^{-3}, showing that Mc Whirter's criteria is fulfilled for all samples, thus satisfying the LTE condition. Comparison of Te and N_e for all tobacco and its ash samples is given in Table 2.

Table 2. Comparison of T_e and N_e in all samples

Sr.No.	*Sample*	*Electron Temperature T_e, K*	*Electron Number Density N_e, 10^{16} cm^{-3}*
1.	S_1	8728.56	3.065
2.	S_2	8728.56	3.065
3.	S_3	8860.80	1.738
4.	S_4	8860.80	1.738
5.	S_5	8928.97	3.003
6.	S_6	8928.97	3.003
7.	S_7	10363.98	1.670
8.	S_8	10363.98	1.670

3.4. Comparison

Chromium, a highly toxic metal, was found in all the samples, posing a significant health risk to consumers. Many different elements have been detected in both tobacco and ash samples among which some are light and some are heavy metals. In gold flake and gold leaf all the detected elements are same and elements detected in capstan and morven are same. The element nickel Ni present in both capstan and morven tobacco while it is not found in gold flake and gold leaf.

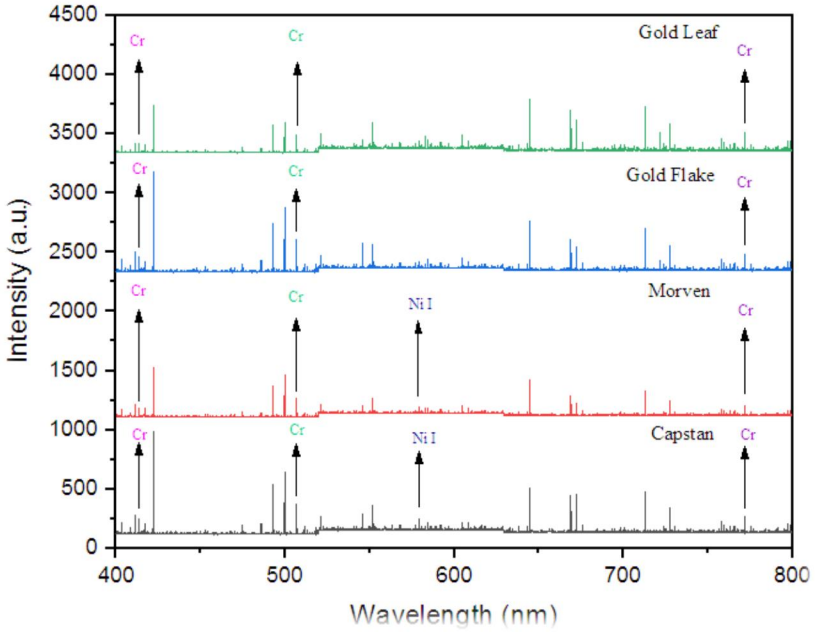

Fig.9.Comparison of different elements in tobacco samples

In ash samples different elements are detected. The ash samples of capstan and morven same elements have been detected whereas, same elements are found in the ash samples of gold flake and gold leaf.

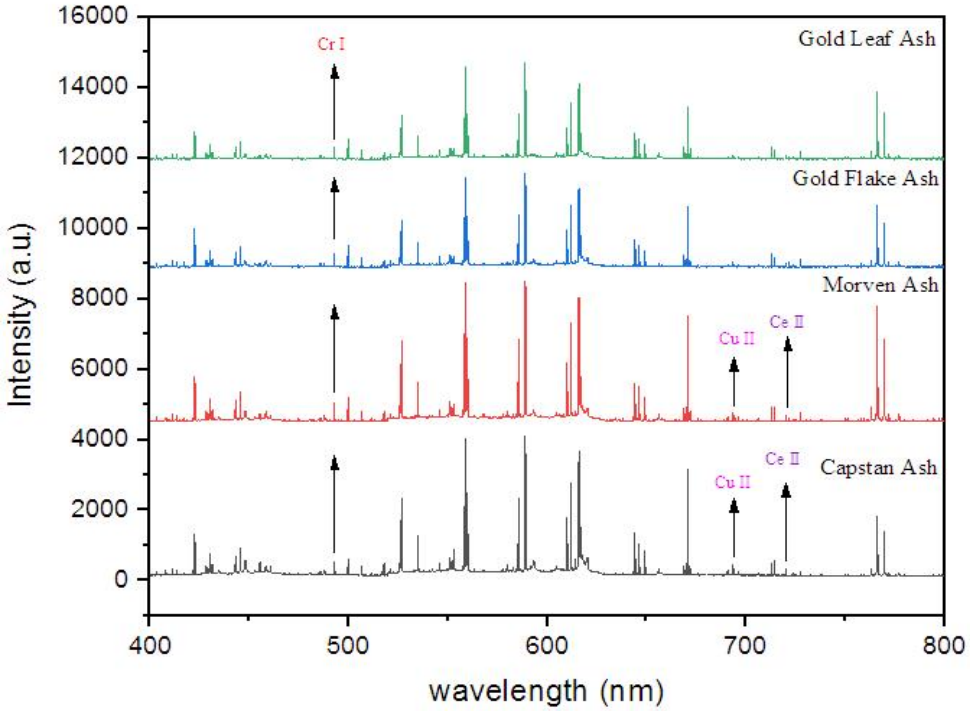

Fig.9.Comparison of different elements in tobacco samples

More elements are detected in ash then in tobacco it may be due to the contribution of metallic elements from cigarette wrapping paper. Our findings have significant implications, highlighting the need to

implement stricter regulations to protect human health and prevent environmental contamination. Furthermore, LIBS technology can be a valuable tool in promoting environmental sustainability by enabling rapid and accurate monitoring of pollutants in soil, water, and air.

4. Conclusions

In this work, different elements from tobacco and its ash have been successfully detected among which some are light and some are heavy metals. Some toxic elements are also present which are not good for human health such as chromium, nickel and strontium. In all the four tobacco samples chromium is present which is highly toxic metals. In tobacco samples S_1 and S_2 nickel is also detected. Presence of chromium is also found in all ash samples. More elements are detected in ash samples then in tobacco samples, it may be due to the contribution of metallic elements from cigarette wrapping paper.

This work shows that LIBS technique could be effectively used to find toxic elements present in cigarettes and their ash. These results can also be used to detect the hazardous elements present in beverages and all other food items. Other materials such as soil, rocks and water can also be investigated.

In conclusion, our study successfully detected various elements, including toxic heavy metals, in tobacco and ash samples using the LIBS technique. The presence of these elements constitute significant health risks, highlighting the need for stricter regulations and monitoring. Our findings have far-reaching implications for human health, agriculture, and environmental sustainability, and we hope that this research will inform future studies and initiatives aimed at reducing the harmful effects of tobacco and its byproducts.

Competing Interests

The authors declare neither present nor potential conflict of interest with the study reported here

Credit Author Statement

Ethical Approval

Not applicable.

Consent to Participate and Publish

Not applicable.

Availability of data and materials

The data sets used and analyzed during the study are available from the corresponding author upon reasonable request.

REFERENCES

[1] X.Y. SAI, F. GAO, W.Y. ZHANG, M. GAO, J. YOU, Y.J. SONG, T.G. LUO, Y.Y. SUN, Combined Effect of Smoking and Obesity on Coronary Heart Disease Mortality in Male Veterans: A 30-year Cohort Study, Biomed. Environ. Sci. 34 (2021) 184–191. https://doi.org/10.3967/bes2021.012.

[2] N. Latif, S.A. Naroo, Transient effects of smoking on the eye, Contact Lens Anterior Eye.45(2022).https://doi.org/10.1016/j.clae.2022.101595.

[3] Q. Zhang, Y. Liu, W. Yin, Y. Yan, L. Li, G. Xing, The in situ detection of smoking in public area by laser-induced breakdown spectroscopy, Chemosphere. 242 (2020). https://doi.org/10.1016/j.chemosphere.2019.125184.

[4] D.C. Colston, Y. Xie, M.E. Patrick, J.F. Thrasher, A.R. Titus, M.R. Elliott, D.T. Levy, N.L. Fleischer, Tobacco 21 laws may reduce smoking and tobacco-related health disparities among youth in the U.S, Prev. Med. Reports. 27 (2022). https://doi.org/10.1016/j.pmedr.2022.101762.

[5] J. Zhang, C. Li, G. Li, Y. He, J. Yang, J. Zhang, Effects of biochar on heavy metal bioavailability and uptake by tobacco (Nicotiana tabacum) in two soils, Agric. Ecosyst. Environ. 317 (2021). https://doi.org/10.1016/j.agee.2021.107453.

[6] J. Yang, J. Wang, X. Liao, H. Tao, Y. Li, Chain modeling for the biogeochemical nexus of cadmium in soil–rice–human health system, Environ. Int. 167 (2022). https://doi.org/10.1016/j.envint.2022.107424.

[7] H. Wu, Q. Liu, J. Ma, L. Liu, Y. Qu, Y. Gong, S. Yang, T. Luo, Heavy Metal(loids) in typical Chinese tobacco-growing soils: Concentrations, influence factors and potential health risks, Chemosphere. 245 (2020).https://doi.org/10.1016/j.chemosphere.2019.125591.

[8] J. Ren, Y. Zhao, K. Yu, LIBS in agriculture: A review focusing on revealing nutritional and toxic elements in soil, water, and crops, Comput. Electron. Agric. 197 (2022). https://doi.org/10.1016/j.compag.2022.106986.

[9] Y. Ling, F. Luo, S. Zhu, A simple and fast sample preparation method based on ionic liquid treatment for determination of Cd and Pb in dried solid agricultural products by graphite furnace atomic absorption spectrometry, Lwt. 142 (2021). https://doi.org/10.1016/j.lwt.2021.111077.

[10] K.B.S. Perelonia, K.C.D. Benitez, R.J.S. Banicod, G.C. Tadifa, F.D. Cambia, U.M. Montojo, Validation of an analytical method for the determination of cadmium, lead and mercury in fish and fishery resources by graphite furnace and Cold Vapor Atomic Absorption Spectrometry, Food Control. 130 (2021).https://doi.org/10.1016/j.foodcont.2021.108363.

[11] H. Lin, K. Uosaki, H. Noguchi, Lithiation of the crystalline silicon as analyzed using soft X-ray emission spectroscopy and windowless energy dispersive X-ray spectroscopy, Appl. Surf. Sci. 569 (2021). https://doi.org/10.1016/j.apsusc.2021.151040.

[12] N. Ahmed, Z.A. Umar, R. Ahmed, M. Aslam Baig, On the elemental analysis of different cigarette brands using laser induced breakdown spectroscopy and laser-ablation time of flight mass spectrometry, Spectrochim. Acta Part B At. Spectrosc. 136 (2017) 39–44. https://doi.org/10.1016/J.SAB.2017.08.006.

[13] I. Zinicovscaia, D. Grozdov, N. Yushin, A. Safonov, I. Proshin, M. Volkov, A. Pryadka, V. Belyaev, E. Shubralova, O. Tsygankov, Analysis of the rolled cotton cloth fixed on the outer surface of the International Space Station using neutron activation analysis and complementary techniques, Acta Astronaut. 189 (2021) 278–282. https://doi.org/10.1016/j.actaastro.2021.08.052.

[14] T.L. Nguyen, A. Anam, F.H. Megbes, I.M. Mohammed, A.S. Abed, A.I. Mallhi, M.A. Alzubaidi, A.A. Amir, A. Ayub, M. Arshad, A. Rauf, H.H.P. Thi, Structural Diversity, Spectral Data and Pharmacological Effects of Genus Nigella, Chem. Biodivers. (2023) e202300037. https://doi.org/10.1002/CBDV.202300037.

[15] E. Vagena, K. Theodorou, S. Stoulos, Thick-foils activation technique for neutron spectrum unfolding with the MINUIT routine—Comparison with GEANT4 simulations, Nucl. Instruments Methods Phys. Res. Sect. A Accel. Spectrometers, Detect. Assoc. Equip. 887 (2018) 64–69. https://doi.org/10.1016/j.nima.2018.01.025.

[16] Z. Hu, D. Zhang, W. Wang, F. Chen, Y. Xu, J. Nie, Y. Chu, L. Guo, A review of calibration-free laser-induced breakdown spectroscopy, TrAC - Trends Anal. Chem. 152 (2022). https://doi.org/10.1016/j.trac.2022.116618.

[17] L. Jiang, M. Sui, Y. Fan, H. Su, Y. Xue, S. Zhong, Micro-gas column assisted laser induced breakdown spectroscopy (MGC-LIBS): A metal elements detection method for bulk water in-situ analysis, Spectrochim. Acta - Part B At. Spectrosc. 177 (2021). https://doi.org/10.1016/j.sab.2021.106065.

[18] A. Hayat, S. Bashir, M.S. Rafique, R. Ahmed, M. Akram, K. Mahmood, A. Zaheer, T. Hussain, A. Dawood, Spatial confinement effects employed by metallic blocker and Ar gas pressures on laser-induced breakdown spectroscopy and surface modifications of laser-irradiated Mg, Laser Part. Beams. 35 (2017) 313–325.https://doi.org/10.1017/S0263034617000210.

[19] M. Akhtar, A. Jabbar, S. Mehmood, N. Ahmed, R. Ahmed, M.A. Baig, Magnetic field enhanced detection of heavy metals in soil using laser induced breakdown spectroscopy, Spectrochim. Acta - Part B At. Spectrosc. 148 (2018) 143–151. https://doi.org/10.1016/j.sab.2018.06.016.

[20] K. Zehra, S. Bashir, S.A. Hassan, Q.S. Ahmed, M. Akram, A. Hayat, The effect of nature and pressure of ambient environment on laser-induced breakdown spectroscopy and ablation mechanisms of Si, Laser Part. Beams. 35 (2017) 492–504. https://doi.org/10.1017/S0263034617000477.

[21] H. Iftikhar, S. Bashir, A. Dawood, M. Akram, A. Hayat, K. Mahmood, A. Zaheer, S. Amin, F. Murtaza, Magnetic field effect on laser-induced breakdown spectroscopy and surface modifications of germanium at various fluences, Laser Part. Beams. 35 (2017) 159–169.https://doi.org/10.1017/S0263034617000039.

[22] S. Fareed, K. Siraj, S. ul Haq, Z. Ahmad, R. Ahsen, R.A. Awan, M.S.A. Rahim, Q. Younas, Identification of Chemical Elements in Tea Leaves and Calculation of Plasma Parameters using Laser-Induced Breakdown Spectroscopy (LIBS), Instruments Exp. Tech. 63 (2020) 744–749. https://doi.org/10.1134/S0020441220050115.

[23] S. Mushtaq, K. Siraj, M.S. Abdul Rahim, S. Ulhaq, Q. Younas, W. Asad, N. Shahzad, A. Latif, Magnetic-Field-Confined Laser Induced Kohl Plasma: Elemental Analysis and Plasma Characterization, Appl. Spectrosc. (2023). https://doi.org/10.1177/00037028231153405.

[24] M.A. Gondal, Y.B. Habibullah, U. Baig, L.E. Oloore, Direct spectral analysis of tea samples using 266 nm UV pulsed laser-induced breakdown spectroscopy and cross validation of LIBS results with ICP-MS, Talanta. 152 (2016) 341–352. https://doi.org/10.1016/j.talanta.2016.02.030.